ORIGINAL ARTICLE

Surface modified nanocrystalline Cr₂O₃ based thick films for gas sensing

Chandak PM ¹, Raghuwanshi FC ², Kapse VD ³ and Kalyamwar VS⁴

¹ Department of Physics, B.B. Arts, N.B. Commerce and B.P. Science College, Digras-445203, Maharashtra State, India

² Department of Physics, Vidyabharati Mahavidyalaya, Amravati-444602, Maharashtra State, India

³ Department of Physics, Arts, Science and Commerce College, Chikhaldara-444807, Maharashtra State, India

⁴ Department of Physics, Bharatiya Mahavidyalaya, Amravati-444605, Maharashtra State, India

Manuscript Details

Cite this article as:

ABSTRACT

Nanocrystalline Cr₂O₃ based thick films were successfully synthesized by co-precipitation method. As synthesized Cr₂O₃ were examined with the help of field emission scanning electron microscopy (FESEM) and energy dispersive X-ray (EDX) spectroscopy. Structural behaviour of Cr₂O₃ nanoparticles was examined by X-ray diffraction (XRD). . Thick films of pure Cr₂O₃ were prepared by screen-printing technique. The surfaces of these films were modified by dipping them into a 0.01M aqueous solution of ferric chloride (FeCl₃) for different intervals of time, followed by firing at 550 ⁰C for 30 min. Gas sensing properties of pure and modified Cr₂O₃ thick films were investigated. Fe₂O₃ modified Cr₂O₃ thick film dipped for 2 min showed higher gas response at 100⁰C. The effect of surface microstructure and Fe₂O₃ concentrations on the gas response, selectivity, response and recovery of the sensor in the presence of NH₃, Cl₂, LPG, CO₂, H₂S and C₂H₅OH gases ware studied and discussed. The quick response and fast recovery are the main features of this sensor.

Keywords: Nanocrystalline; Chromium Oxide; Thick films; Additives

1. INTRODUCTION

The releases of various chemical pollutants from industries, automobiles and homes into atmosphere have been causing the global environmental issues such as the global greenhouse effect, acid rain and ozone depletion. The metal oxides based semiconductor gas sensors are playing an important role in the detection of toxic pollutants in air and to control the industrial processes. It is observed that when the sensors are exposed to the atmosphere, the chemical species to be detected in the atmosphere

can enter in to the interface of the p-n junction. So there are changes in electrical properties at the junction [1-3]. So the gas sensors have been fabricated using, ZnO SnO_2, TiO_2, WO_3, Cr_2O_3, etc. materials in pure and modified forms to detect toxic, harmful, flammable and explosive gases [4,5]. Among different chromium oxide solid phases, Cr_2O_3 is the most stable, existing in a wide range of temperature and pressure [6]. The Cr_2O_3 is a very useful material because of its high melting temperature ($\sim$ 2300^{0}C) and has a Hexagonal-Rhombic corundum crystal structure showing p-type semiconductivity. In the recent years, p-type Cr_2O_3 is gaining importance for sensor applications as it has an energy band gap of ~3.4 eV and widely been used in variety of applications, such as, catalytic reactions, optical coating and infrared sensors [7–10].

It has been observed that, semiconducting oxides such as ZnO, SnO_2, Cr_2O_3, Fe_2O_3 and $BaTiO_3$ [11-22] are sensitive to various polluting toxic gases. It is studied that Cr_2O_3 [23-26] is used as a gas-sensing materials. Cr_2O_3 is the transition-metal oxide. As we know that the transition-metal oxides are more sensitive to the change of outside ambient and these types of oxides could be more preferable for the use in gas sensors [27]. It has been found that a pure Cr_2O_3 thick film has poor gas sensitivity to reducing gases but Fe_2O_3 modified Cr_2O_3 thick film is the most sensitive to LPG, C_2H_5OH, NH_3 and Cl_2 gases [25].

The most advantage of nanotechnology is not only in the small size of nanoparticles but also to exhibit exceptional properties due to their reduced size. As the reduction of particles take place, the specific surface area increases with decrease in particle size. The increase in the specific surface area is unique properties of the nanoparticles from the bulk material with the change in the surface properties of the particles itself. The particle size plays an important role in gas sensing. The reduction in grain-size is one of the prominent factors for enhancing the gas sensing properties of semiconducting oxides.

Many preparation techniques for synthesis of Cr_2O_3 nanoparticles are described, such as hydrothermal reduction [28], solid thermal decomposition [29], urea method [30], and mechanochemical reaction [31]. In present work, co-precipitation methods (chemical route methods) were adopted, as they are easy, suitable and economically low coast to synthesize Cr_2O_3 nanostructures. Moreover the chemical precipitation is considered as a one step synthesis and a less time consuming method. In this method, homogeneous mixing of the reactant precipitates reduces the reaction temperature.

Ammonia is extensively used in many fertilizer factories, chemical industries, refrigeration systems, etc. A leak in the system is harmful for the health hazards. Ammonia is toxic in nature. The leakage of ammonia causes chronic lung disease, irritating and even burning the respiratory track, etc. It is therefore, necessary to detect ammonia gas.

The aim of the present work is to develop the ammonia sensor by modifying pure Cr_2O_3 thick films, which is able to detect ammonia at trace levels. Among the various metal oxide additives tested, Fe_2O_3 is outstanding in promoting the sensing properties of the Cr_2O_3 sensor foe ammonia. The present paper reports the structure, morphology and gas sensing properties of Pure and modified Cr_2O_3 based thick films.

2. EXPERIMENTAL DETAILS

2.1. Preparation of Nanocrystalline Cr_2O_3 Powders

All chemicals were of analytical grade and used directly without further purification. Nanocrystalline Cr_2O_3 powders were synthesized by chemical precipitation method. In present work, 25·50gm Cr $(NO_3)_3$·9H_2O was dissolved in 50 ml double distilled water and then kept on magnetic stirrer at 80°C for 1 h, a transparent solution was formed. In this solution ammonia was added drop wise with constant stirring until the optimum pH of solution becomes 9. After complete precipitation, the hydroxide was washed with double distilled water and ethanol, followed by drying at 110^{0}C for 24 h. Cr_2O_3 nanomaterial was obtained by calcining chromium hydroxide at 500^{0}C and 600^{0}C for 5 h. The synthesized Cr_2O_3 nanostructure product was used for further study.

2.2. Preparation of thick films

Thick films of Cr_2O_3 nanostructure were prepared by using screen printing technique. In this process thixotropic paste was formulated by mixing the synthesized Cr_2O_3 nanostructure powder with ethyl cellulose (a temporary binder) in mixture of three organic solvents such as butyl cellulose, butyl carbitol acetate and turpineol. The ratio of Cr_2O_3 to ethyl cellulose was kept 95:05. The ratio of inorganic to

organic part was kept as 75:25 in formulating the pastes. The ready thixotropic pastes were screen printed on a glass substrate in desired patterns. The films prepared were fired at 500^0C for 12 h. Prepared thick films termed as pure Cr_2O_3 thick films.

2.3. Fe_2O_3 modified Cr_2O_3 thick films

Surface of pure Cr_2O_3 thick films were modified by dipping them into 0.01M aqueous solution of $FeCl_3$ (99%ARgrade, Merck) for different intervals of time (2 and 4 min). Dipped thick films were dried under IR lamp for 1 h. Dried thick films were fired at 500^0C for 30 min. The $FeCl_3$ dispersed on the film surface was oxidised to Fe_2O_3 in firing process and sensor elements with different mass % of Fe_2O_3 on the surface of Cr_2O_3 thick films were obtained. These surface modified thick films are termed as Fe_2O_3 modified Cr_2O_3 thick films.

3. RESULTS AND DISCUSSION

3.1. X-ray diffraction

The crystallographic structure of the synthesized Cr_2O_3 nanostructure was characterized by powder x-ray diffraction with Cu-Kα source and 2θ range of 20-80⁰. Fig. 1 shows X-ray diffraction (XRD) pattern of synthesized pure Cr_2O_3 powder sample. The observed peaks are matching well with JCPDS reported data of pure Cr_2O_3 (JCPDS card no.70-3766). The characteristic peaks observed in the spectrum are higher in intensity which indicates that the as-synthesized samples are of good crystalline in nature. The XRD spectrum confirms that, the powder is nanocrystalline in nature and hexagonal in structure.

The domain size of the crystal can be estimated from the full width at half maximum (FWHM) of the peaks by means of the Scherrer formula [32].

The average crystallite size (D) was estimated from the Debye–Scherrer's equation:

$$D = 0.9\,\lambda\ /\ \beta\ Cos\ \theta$$

where λ is the wavelength of X-rays (1.54056 Å), β is the FWHM of the peak in radians, θ is the diffraction angle at which the full width at half maximum (FWHM) measured and   k =0.9, is Scherrer constant.

The average crystallite size of the synthesized Cr_2O_3 nanoparticles calculated from (110) peak was approximately 26 nm.
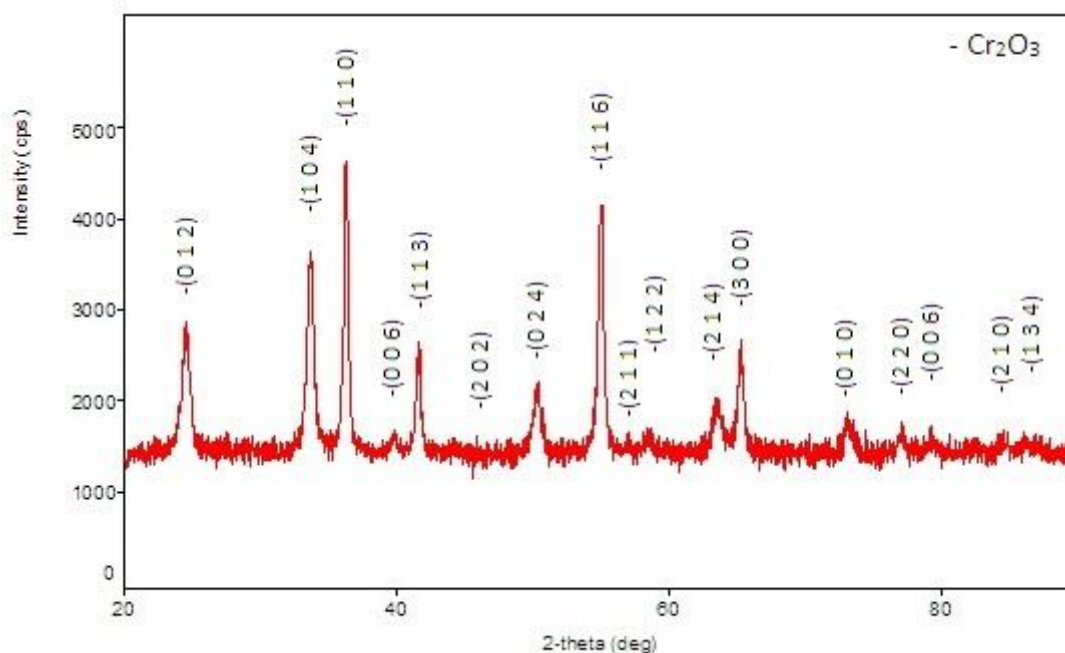

Fig. 1: X-ray diffraction pattern of Cr_2O_3 powder sample calcinated at 500 ^0C.

3.2 Scanning electron microscopy

3.2.1 Pure Cr$_2$O$_3$ film

Fig. 2 shows the FE-SEM image of the pure Cr$_2$O$_3$ film. It consists of randomly distributed grains with larger size and shape distribution. The average size of Cr$_2$O$_3$ grains are approximately 37 nm. The appearance of the film looks porous, which supports the adsorption and desorption type of gas sensing mechanism. The nano scaled grains exhibit high surface to volume ratio.

3.2.2 Fe$_2$O$_3$ modified Cr$_2$O$_3$ thick films

Fig. 3 (a-b) shows typical FE-SEM images of Fe$_2$O$_3$ modified Cr$_2$O$_3$ thick films prepared by screen printing technique. Fig. 3 (a) depicts the microstructure of Fe$_2$O$_3$ modified Cr$_2$O$_3$ thick film for 2 min, consist of particles with smaller size and shape associated with the Cr$_2$O$_3$ grains with sizes ranging from 20 nm to 30 nm distributed non-uniformly. This film looks porous (not masked) after activation, increasing surface to volume ratio as well as gas response.

Fig. 3 (b) depicts the microstructure of Fe$_2$O$_3$ modified Cr$_2$O$_3$ thick film for 4 min, consists of large number of smaller grains of Fe$_2$O$_3$ in association with Cr$_2$O$_3$. The film consists of grains with sizes ranging from 18 nm to 27 nm distributed non-uniformly. The film is masked reducing surface to volume ratio as well as gas response. Moreover, it can be seen that there is decrease in the agglomerations with the increase in the content of Fe. The average grain size of the fabricated thick films is observed to be in the range of 20 nm to 36 nm.
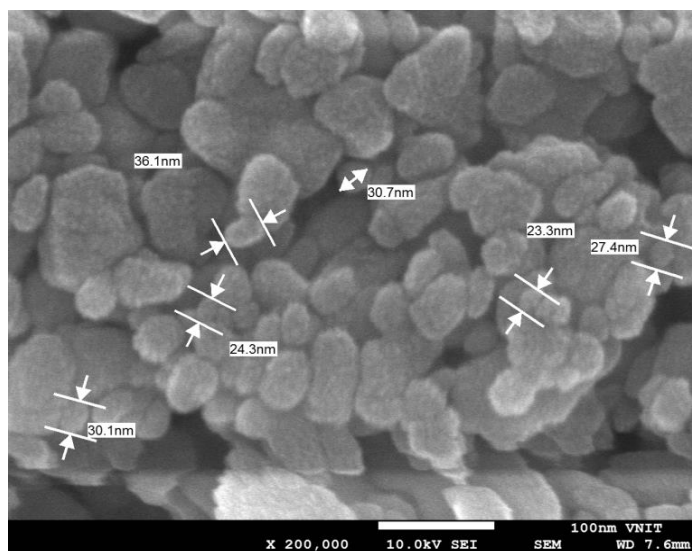

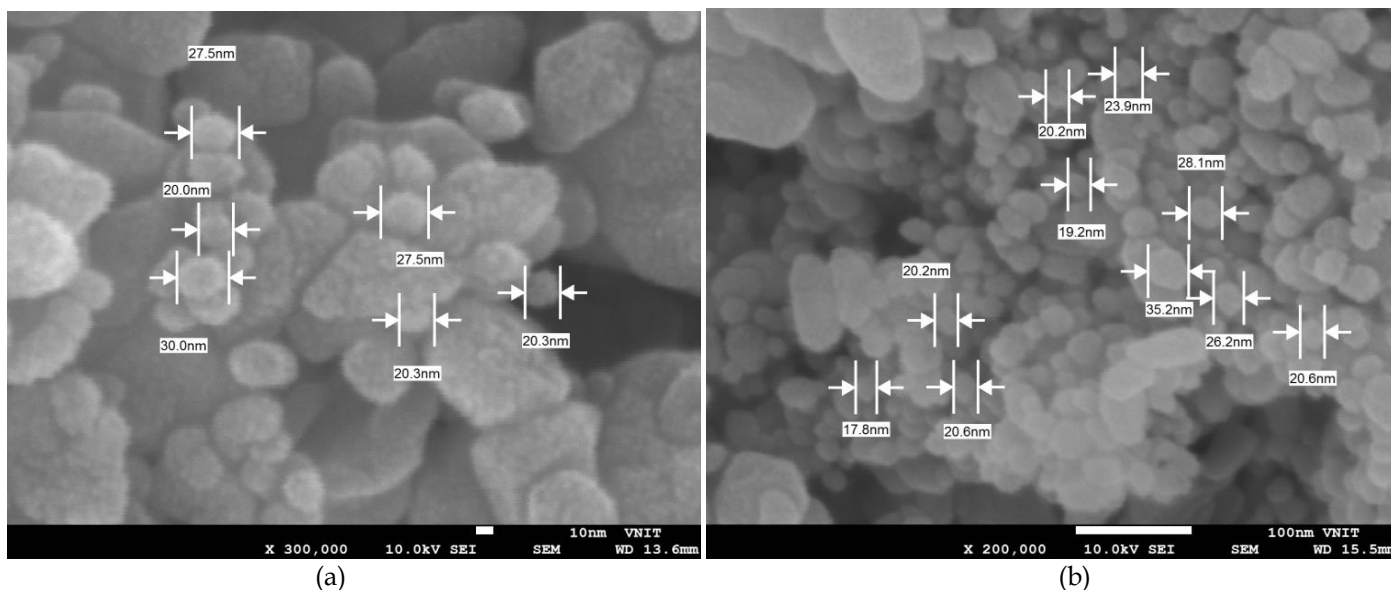**Fig. 2: FE-SEM microstructures for pure Cr$_2$O$_3$ thick film**

(a)   (b)

Fig. 3: FE-SEM microstructures for : (a) Fe$_2$O$_3$ modified Cr$_2$O$_3$ thick film (2 min) *(b) Fe$_2$O$_3$ modified Cr$_2$O$_3$ thick film (4 min).*

3.3 Quantitative Elemental Analysis (EDX)

The quantitative elemental composition of the pure and Fe_2O_3 modified Cr_2O_3 thick films were analyzed using an Energy Dispersive Spectrometer (EDS). Fig.4 (a-c) illustrates the EDS patterns of pure and Fe_2O_3 modified thick films with different dipping times. These figures indicate that as the dipping time increases intensity of Fe peak increases, which indicate the increasing in mass percentage of Fe on the surface of the Cr_2O_3 thick film.
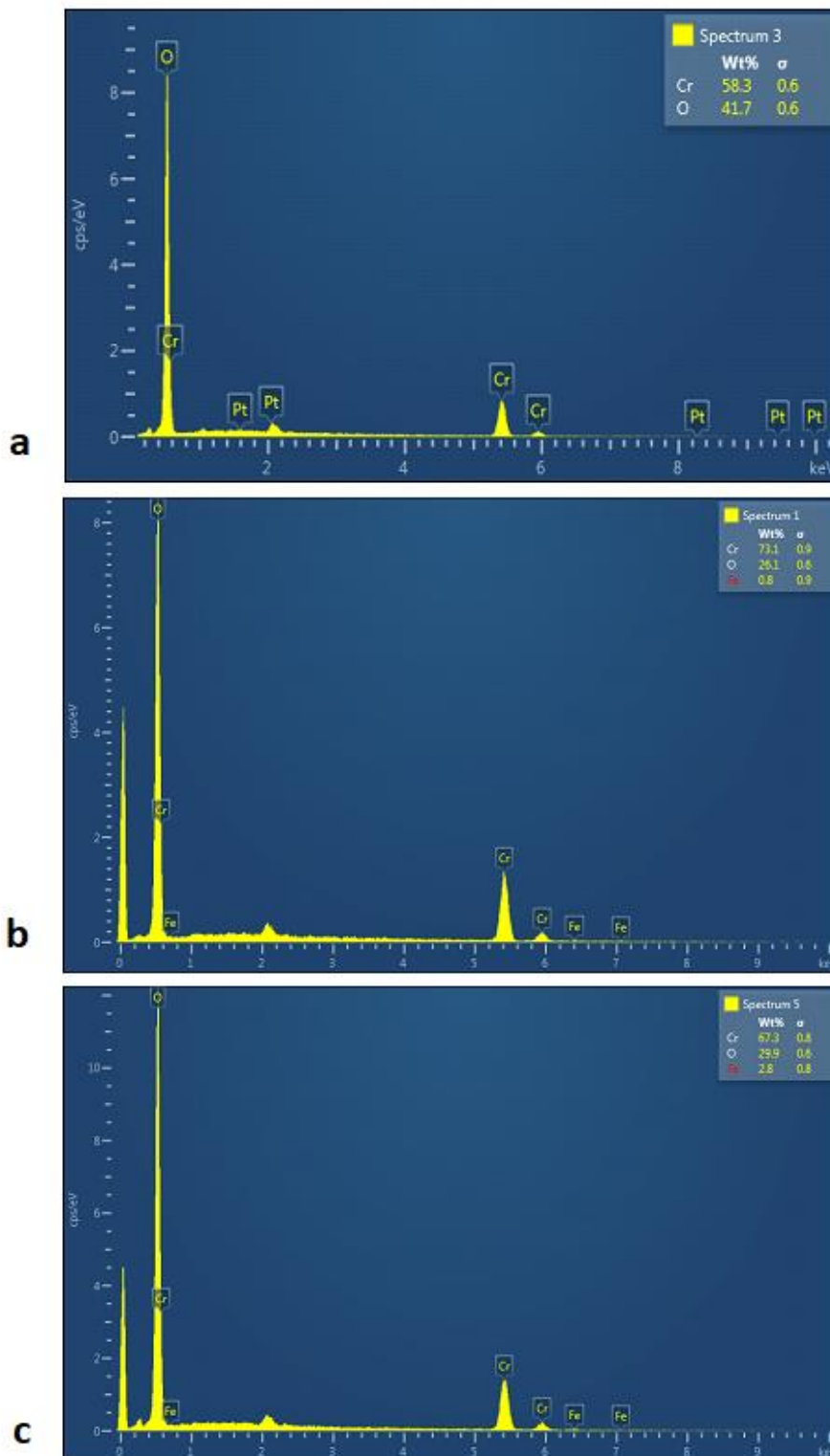

***Fig.4: EDS patterns for a) pure Cr₂O₃ thick film b) Fe₂O₃modified Cr₂O₃ (2 min dip.)
c) Fe₂O₃modified Cr₂O₃ thick film (4 min dip.)***

**Table 3.1: Mass % of Cr, O and Fe elements in pure and modified thick films**

Sample	Pure Cr$_2$O$_3$	Fe$_2$O$_3$ modified Cr$_2$O$_3$ thick films (with different dipping time)	
Element		2min.	4min
O	41.7	26.1	29.9
Cr	58.3	73.1	67.3
Fe	-	0.8	2.8

It is clear from Table 3.1 that, as the dipping time increases the mass % of Fe$_2$O$_3$ on the surface of the film increases which may be attributed to the chemisorptions of ferric chloride particles on the surface of the thick films proving masking of the film during dipping process. Thus, dipping process is the simple and low cost technique to activate the surface of the film. This forms heterojunctions on the surface of the film which increases the resistivity.

3.4 Electrical Performance of the Sensor

3.4.1 I-V characteristics

Current was measured with increasing bias voltage in the step of 5V from 0 to 30 V.The measurement was repeated with negative voltage. The symmetrical natures of the I-V characteristics for particular samples show that the contacts are ohmic in nature. Fig. 5 also shows that the conductivity of pure Cr$_2$O$_3$ film is larger than Fe$_2$O$_3$ modified Cr$_2$O$_3$ thick films.
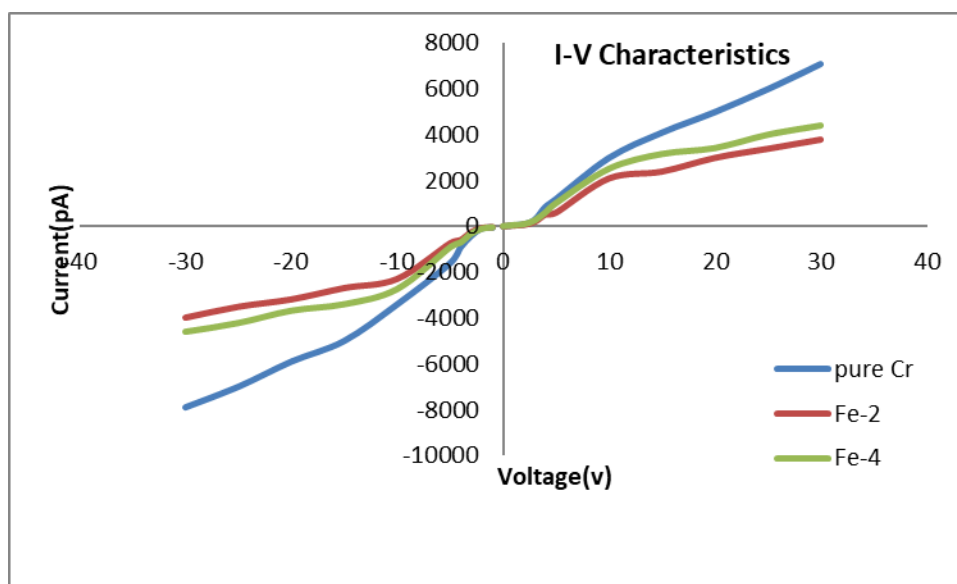
Fig.5: I-V characteristics of pure and Fe$_2$O$_3$ modified Cr$_2$O$_3$ thick films at room temperature.

3.5 Gas Sensing Performance of the Sensor

3.5.1 Unmodified (Pure) Cr$_2$O$_3$ and Fe$_2$O$_3$ modified Cr$_2$O$_3$ thick films.

Fig. 6 depicts the gas response of pure and Fe$_2$O$_3$ modified Cr$_2$O$_3$ thick films as a function of operating temperature. The gas response of pure and Fe$_2$O$_3$ modified Cr$_2$O$_3$ thick films to 100 ppm NH$_3$ were investigated at various operating temperatures ranging from room temperature to 400^{0}C.

From figure it is clear that gas response and operating temperature are influenced by different dipping times. Fig. 6 also shows the variation of gas response of a pure Cr$_2$O$_3$ thick film with operating temperature to 100 ppm NH$_3$ gas. The response to NH$_3$ gas goes on increasing with operating temperature, reaches to a maximum at 100^{0}C and decreases with the further increase of operating temperature. As we know that, response to a NH$_3$ gas is generally depends on the number of oxygen ions adsorbed on the surface of the film with a target

gas. If the film surface chemistry was favourable for adsorption, response and selectivity would be enhanced. In the case of pure Cr_2O_3 thick film, oxygen adsorption seems to be poor and not easier which could be the reason for poor response to NH_3. In addition to this, the gas may burn before reaching the surface and therefore it would respond at higher operating temperature. So, to improve the sensing performance of pure Cr_2O_3, it is essential to modify pure Cr_2O_3.

It is also clear from figure that Fe_2O_3 modified Cr_2O_3 thick film at 2 min dipping time gives highest response to 100 ppm NH_3 at 100^0C as compared to 4 min dipped thick film, it may be attributed to the amount of Fe_2O_3 grains over Cr_2O_3 grains are suitable. When the optimum amount of Fe_2O_3 (2 min dipping) is dispersed on the surface of Cr_2O_3 thick film, the Fe_2O_3 grains would be distributed uniformly throughout the surface film. These Fe_2O_3 grains form potential barrier (p-n heterojunctions) with Cr_2O_3. Due this potential barrier, sensor element offers high resistance. So, such amount of high resistance would be sufficient to promote the catalytic reaction effectively. These overall changes lead to high gas response when this type of sensor element expose to NH_3 gas.

3.5.2 Selectivity

Fig. 7 depicts the selectivity of all, pure and Fe_2O_3 modified Cr_2O_3 thick films towards LPG, C_2H_5OH, CO_2, NH_3, H_2S and Cl_2 for 100 ppm concentration at 100^0C. These modified thick films shows higher selectivity for NH_3 gas among all the gases. It is observed from figure that the 2 min. Fe_2O_3 modified Cr_2O_3 thick film is most sensitive to NH_3 gas at 100^0C among all other tested gas.

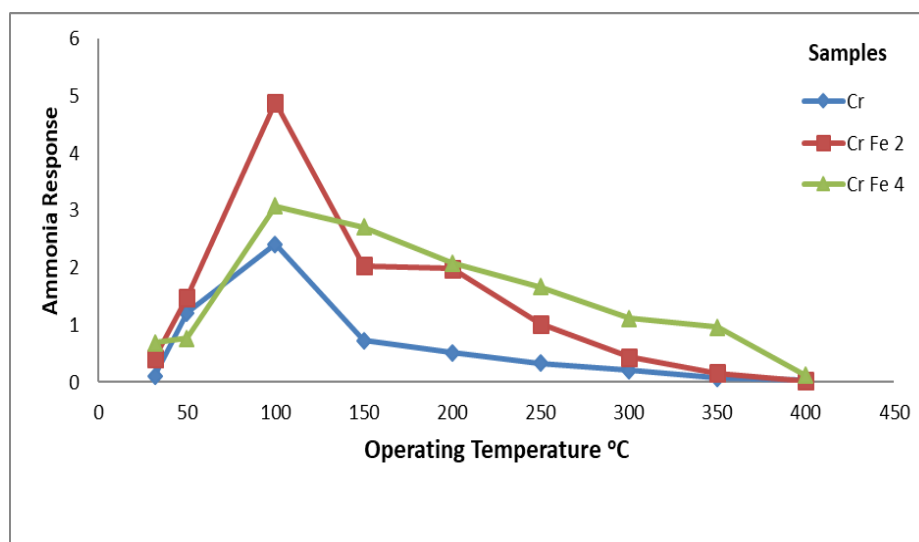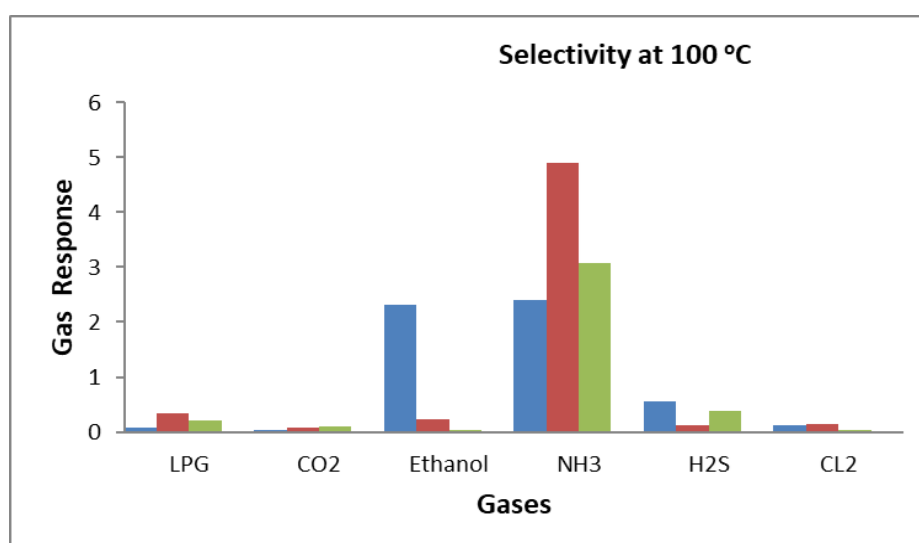**Fig 6: Variation of gas response of pure and Fe_2O_3 modified Cr_2O_3 thick films with operating temperature**

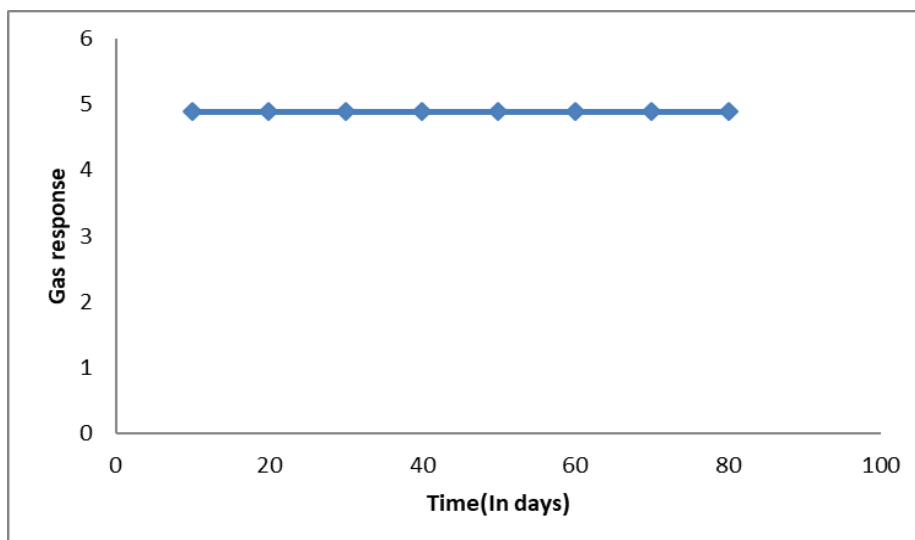*Fig. 7: Selectivity of pure and Fe_2O_3 modified Cr_2O_3 thick films*

Fig. 9: Stability of Fe$_2$O$_3$ modified Cr$_2$O$_3$ thick film (2 min dip.)

3.5.3 Active Nature

Fig. 8 exhibits the relation between gas response of pure and Fe$_2$O$_3$ modified Cr$_2$O$_3$ thick films and concentration of NH$_3$ gas at100^{0}C.It is clear from the figure that the gas response of Fe$_2$O$_3$ modified Cr$_2$O$_3$ thick film (2 min dipping) increases linearly with gas concentration up to 100 ppm. The rate of increase in response was relatively larger up to 100 ppm and saturated beyond 100 ppm. The active region for the ammonia sensor is up to 100 ppm. So, for proper functioning, the sensor should work in the active region only.

3.5.4 Response and Recovery time

The response and recovery of the Fe$_2$O$_3$ modified Cr$_2$O$_3$ thick film (2 min dipped) to 100 ppm of NH$_3$ are 10 s and 14 s respectively. Thus the sensor showed very rapid response and recovery time to NH$_3$ gas. For better performance of the sensor the recovery should be very fast. When the gas exposure was switched off, the sensor returned back to its original chemical status, within very short time (14 s). This is the main feature of this sensor.

3.5.5 Stability

Fig.9 depicts NH$_3$ gas response over a long time duration for Fe$_2$O$_3$ modified Cr$_2$O$_3$ thick film (3 min. dipped) to 100 ppm of NH$_3$.The response of this sensor towards 100 ppm of NH$_3$ gas at 100^{0}C was measured for two month in the interval of 10 days as shown in figure. Thus the sensor showed a very stable response confirming the stability and hence reproducibility of the material.

3.5.6 Gas sensing mechanism

The working principle of thick film semiconducting gas sensors is based on the change of the electronic conductivity of the semiconducting material on exposure of target gas. In such mechanism, the atmospheric oxygen molecules O$_2$ (air) are adsorbed on the surface of the thick film. They capture the electrons from the conduction band of the thick film material as:

$$O_{2\,(air)} \; + \; 4\,e^-_{(cond.band)} \; \rightarrow \; 2\,O^{2-}_{(film\,surface)}$$

It would result in decreasing conductivity of the film.As we know that, the lone pair of electrons of NH$_3$ provides strong electron acceptor behaviour. But it acts as an electron donor to the metal oxide, when reacted with the adsorbed oxygen ions on the surface by returning the trapped electrons to conduction band. The reactions that generates free electrons when the number of oxygen ions reacted with NH$_3$ molecules, given in the following equations [33].

$$4NH_3 + 3O_{2\,(adsorbed)} \rightarrow 6H_2O + 2N_2 + 6e-$$

Or

$$2NH_3 + 3O^-_{(adsorbed)} \rightarrow 3H_2O + N_2 + 3e-$$
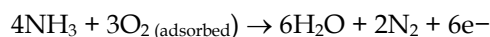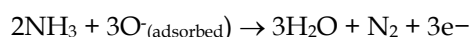
Upon exposure, ammonia molecules react with adsorbed oxygen on the surface of the film got oxidized to nitrogen oxide gas and water vapors as the products liberating free electrons in the conduction band.

4. CONCLUSIONS

The results of pure and Fe_2O_3 modified Cr_2O_3 thick films can be summarized as follows

1. The pure Cr_2O_3 film was more conductive than all Fe_2O_3 modified Cr_2O_3 thick film

2. In case of surface modified thick films (4 min dip.) Fe_2O_3 modified Cr_2O_3 thick film showed higher conductivity.

3. A pure Cr_2O_3 thick film was almost insensitive to all tested reducing gases.

4. Fe_2O_3 modified Cr_2O_3 thick film (2 min dip) showed higher gas response to 100 ppm NH_3 gas at 100^0C.

5. The sensor showed good selectivity to NH_3 gas against Cl_2, LPG, CO_2, H_2S and C_2H_5OH gases at 100^0C.

6. The sensor showed very rapid response and recovery time to NH_3 gas.

REFERENCES

1. Choi JD, Choi GM, Electrical and CO gas sensing properties of layered ZnO–CuO sensor, *Sensors and Actuators* B, 2000; 69: 120–126. https://doi.org/10.1016/S0925-4005(00)00519-0.

2. Bae HY, Choi GM. Electrical and reducing gas sensing properties of ZnO and ZnO–CuO thin films fabricated by spin coating method, *Sensors and Actuators* B; 1999; 55: 47–54. https://doi.org/10.1016/S0925-4005(99)00038-6.

3. Jung SJ, Yanagida H. The characterization of a CuO/ZnO heterocontact-type gas sensor having selectivity for CO gas, *Sensors and Actuators* B, 1996; 37: 55–60. https://doi.org/10.1016/S0925-4005(96)01986-7.

4. Shen YB, Wang W, Chen XX, Zhang BQ, Wei DZ, Gao SL, et al., J. Nitrogen dioxide sensing using tungsten oxide microspheres with hierarchical nanorod-assembled architectures by a complexing surfactant-mediated hydrothermal route, *Mater.Chem*. A; 2016; 4: 1345–1352. http://dx.doi.org/10.1039/C5TA08170J.

5. Cui JB, Shi LQ, Xie TF, Wang DJ, Lin YH. UV-light illumination room temperature HCHO gas-sensing mechanism of ZnO with different nanostructures, Sens Actuators B 227 (2016)220–226. https://doi.org/10.1016/j.snb.2015.12.010.

6. Kubota B. Decomposition of Higher Oxides of Chromium Under Various Pressures of Oxygen, *J. Am. Ceram. Soc*. 1961; 44: 239-248. https://doi.org/10.1111/j.1151-2916.1961.tb15368.x.

7. Cantalini C. Cr_2O_3, WO_3, single and Cr/W binary oxide prepared by physical methods for gas sensing application, *J. Eur. Chem. Soc*. 2004; 24: 1421–1424. https://doi.org/10.1016/S0955-2219(03)00442-4.

8. Cellard A, Garnier V, Fantozzi G, Baret G, Fort P. Wear resistance of chromium oxide nanostructured coatings, *Ceram. Int*. 2009; 35:913–916. https://doi.org/10.1016/j.ceramint.2008.02.022.

9. Sahar A. El-Molla, Surface and catalytic properties of Cr_2O_3/MgO system doped with manganese and cobalt oxide, *Appl. Catal. A*; 2005; 280: 189–197. DOI: 10.1016/j.apcata.2004.10.042.

10. Roy Morrison S. Surface states on a chromia catalyst, *J. Catal.* 1997; 47: 69–78. https://doi.org/10.1016/0021-9517(77)90151-8.

11. Chen Z, Colbow K. MgO doped Cr_2O_3: solubility limit and the effect of doping on the resistivity and ethanol sensitivity, *Sens. Actuators* B, 1992; 9:49- 53. https://doi.org/10.1016/0925-4005(92)80192-Z.

12. Patil DR, Patil LA, Jain GH, Wagh MS, Patil SA. Surface activated ZnO thick film resistors for LPG gas sensing, *Sensors and Transducers,* 2006; 74: 874-883.

13. Patil DR, Patil LA. Preparation and study of NH3 gas sensing behaviour of Fe_2O_3 doped ZnO thick film resistors, *Sensors and Transducers*, 2006; 70: 661-670.

14. Shriver DF, Atkins PW, Inorg. Chem. (3rd ed.), Oxford University press, 2004, pp. 184- 190.

15. Sodhi GS. Fundamental concepts of Environmental Chemistry, (1st edition) Narosa Publishing House New Delhi, 2002, pp. 215-302.

16. Ruiz M, Sakai G, Cornet A, Shimanoe K, Morante JR, Yamazoe N. Cr-doped TiO2 gas sensor for exhaust NO_2 monitoring, Sens. Actuators B 2003; 93: 509-518. https://doi.org/10.1016/S0925-4005(03)00183-7.

17. Patil DR, Patil LA. Ammonia sensing resistors based on Fe2O3-modified ZnO thick films, Sensors IEEE 7 (2007) 434-439. DOI: 10.1109/JSEN.2006.886977.

18. Patil DR, Patil LA. Room temperature chlorine gas sensing using surface modified ZnO thick film resistors, *Sens. Actuators* B, 2007; 123" 546-553.

    https://doi.org/10.1016/j.snb.2006.09.060

19. Patil DR, Patil LA. Al_2O_3-modified ZnO based thick film resistors for H_2-gas sensing, *Sensors and Transducers*, 2007; 81: 1354-1363.

20. Jain GH, Patil LA, Wagh MS, Patil DR, Patil SA, Amalnerkar DP. Surface modified $BaTiO_3$ thick film resistors as H_2S gas sensors, *Sens. Actuators* B, 2006;117 : 159-165. https://doi.org/10.1016/j.snb.2005.11.031.

21. Wagh MS, Jain GH, Patil DR, Patil SA, Patil LA, Modified zinc oxide thick film resistors as NH_3 gas sensor, *Sens. Actuators B* 2006; 115 :128-133. https://doi.org/10.1016/j.snb.2005.08.030.

22. Wagh MS, Jain GH, Patil DR, Patil SA, Patil LA. Surface customisation of SnO_2 thick films using RuO_2 as a

surfactant for the LPG response, Sens. Actuators B 122 (2007) 357-364. https://doi.org/10.1016/j.snb.2006.05.014.

23. Jantson T, Avarmaa T, Mandar H, Uustave T, Jaaniso R. Nanocrystalline Cr_2O_3-TiO_2 thin films by pulsed laser deposition, *Sens. Actuators* B, 2005; 109: 24-31. https://doi.org/10.1016/j.snb.2005.03.014.

24. Martin LP, Pham AQ, Glass RS. Effect of Cr_2O_3 electrode morphology on the nitric oxide response of a stabilized zirconia sensor, *Sens. Actuators* B, 2003; 96: 53-60. https://doi.org/10.1016/S0925-4005(03)00485-4.

25. Suryawanshi DN, Patil DR, Patil LA. Fe_2O_3-activiated Cr_2O_3 thick films as temperature dependent gas sensors, *Sens. Actuators* B 134 (2008) 579-584. https://doi.org/10.1016/j.snb.2008.05.045.

26. Shriver DF, Atkins PW. Inorg. Chem.), Oxford University press, 2004, pp. 652 - 627.

27. Patil LA. *Sensors & Transducers Journal*, 2009; 104 (5): 68-75.

28. Pei Z, Xu H, Zhang Y. Preparation of Cr_2O_3 nanoparticles via C_2H_5OH hydrothermal reduction *Journal of Alloys and Compounds*, 2009; 468: L5–L8. https://doi.org/10.1016/j.jallcom.2007.12.086.

29. Li L, Zhu Z, Yao X, Lu G, Yan Z. Synthesis and characterization of chromium oxide nanocrystals via solid thermal decomposition at low temperature *Microporous and Mesoporous Materials*. 2008; 112: 621–626. https://doi.org/10.1016/j.micromeso.2007.10.044.

30. Ocana M. Nanosized Cr_2O_3 hydrate spherical particles prepared by the urea method. *Journal of the European Ceramic Society*; 2001; 21: 931–939. https://doi.org/10.1016/S0955-2219(00)00288-0.

31. Tsuzuki T, Mccormick PG. Synthesis of Cr_2O_3 nano-particles by mechanochemical processing, *Acta Materialia*, 2000; 48: 2795–2801. https://doi.org/10.1016/S1359-6454(00)00100-2.

32. Hilber T, Letonja P, Marr R, Poit P, Siebenhofer M. Formation of Submicron Zinc Particles by Electrodeposition, *Part. Part. Syst. Charact*. 19 (2002) 342-347. https://doi.org/10.1002/1521-4117(200211)19:5<342::AID-PPSC342>3.0.CO;2-6

33. Nguyen T, Park S, Kim JB, Kim TK, Seong GH, Choo J, Kim YS, Beom J,   Kyu T, Hun G, Shin Y. Polycrystalline tungsten oxide nanofibers for gas-sensing applications *Sens. Actuators* B, 2011; 160: 549-554. https://doi.org/10.1016/j.snb.2011.08.028.